Supporting Information

Controlling ethanol use in chain elongation by CO_2 loading rate

Mark Roghair [a], Tim Hoogstad [a], David P.B.T.B. Strik [a,], Caroline M. Plugge [b, c], Peer H.A. Timmers [b, c], Ruud A. Weusthuis [d], Marieke E. Bruins [e], Cees J.N. Buisman [a]*

[a] Sub-department of Environmental Technology, Wageningen University & Research, Bornse Weilanden 9, 6708 WG, Wageningen, the Netherlands
[b] Laboratory of Microbiology, Wageningen University & Research, Stippeneng 4, 6708 WE, Wageningen, the Netherlands
[c] Wetsus, European Centre of Excellence for Sustainable Water Technology, Oostergoweg 9, 8911 MA Leeuwarden, the Netherlands
[d] Bioprocess Engineering, Wageningen University & Research, Droevendaalsesteeg 1, 6708 PB, Wageningen, the Netherlands
[e] Wageningen Food & Biobased Research, Wageningen University & Research, Bornse Weilanden 9, 6708 WG, Wageningen, the Netherlands

* Corresponding author: E-mail: david.strik@wur.nl; tel +31 317 483 447

8 Tables
3 Figures
14 Pages

Table S1. Overview of dominant and considered processes and their corresponding reaction equations. $\Delta G_r^{0\prime}$ values were calculated at standard conditions (25 °C, pH 7.0, liquid components at 1M and gaseous components at 1 atm)

Processes	Organism(s)	Reaction equation	Coupled processes	$\Delta G_r^{0\prime}$ kJ·reaction^{-1}	
1) Processes involved in the carbon flux of ethanol upgrading					
1a) Excessive ethanol oxidation	Ethanol oxidizers	$C_2H_6O + H_2O \rightarrow C_2H_3O_2^- + H^+ + 2H_2$		9.6	
1b) Ethanol oxidation	Chain elongaters	$C_2H_6O + H_2O \rightarrow C_2H_3O_2^- + H^+ + 2H_2$	x1	9.6	**Processes involved in the reverse β-oxidation pathway**
1c) Chain elongation of acetate to butyrate	Chain elongaters	$C_2H_3O_2^- + C_2H_6O \rightarrow C_4H_7O_2^- + H_2O$ [i]	x5	-38.6	
1d) Chain elongation of butyrate to caproate	Chain elongaters	$C_4H_7O_2^- + C_2H_6O \rightarrow C_6H_{11}O_2^- + H_2O$ [i]	x5	-38.8	
1e) Chain elongation of caproate to caprylate	Chain elongaters	$C_6H_{11}O_2^- + C_2H_6O \rightarrow C_8H_{15}O_2^- + H_2O$ [i]	x5	-38.8	
2) Processes involved in the carbon flux of VFA upgrading					
2a) Chain elongation of propionate to valerate	Chain elongaters	$C_3H_5O_2^- + C_2H_6O \rightarrow C_5H_9O_2^- + H_2O$ [i]	x5	-38.6	
2b) Chain elongation of valerate to heptanoate	Chain elongaters	$C_5H_9O_2^- + C_2H_6O \rightarrow C_7H_{13}O_2^- + H_2O$ [i]	x5	-37.1	
3) Processes involved in syntrophic ethanol oxidation					
3a) (Excessive) ethanol oxidation	Chain elongaters & Ethanol oxidizers	$C_2H_6O + H_2O \rightarrow C_2H_3O_2^- + H^+ + 2H_2$ [ii]		9.6	
3b) Hydrogenotrophic methanogenesis	Hydrogenotrophic methanogens	$2H_2 + 0.5CO_2 \rightarrow 0.5CH_4 + H_2O$		-65.3	
3c) Syntrophic ethanol oxidation		$C_2H_6O + 0.5\,CO_2 \rightarrow C_2H_3O_2^- + H^+ + 0.5\,CH_4$	Overall	-55.7	
5) Propionate oxidation	Propionate oxidizers	$C_3H_5O_2^- + 2H_2O \rightarrow C_2H_3O_2^- + 3H_2 + CO_2$		71.7	
6) Homoacetogenesis	Homoacetogens	$2CO_2 + 4H_2 \rightarrow C_2H_3O_2^- + H^+ + 2H_2O$		-95.0	

[i] This process is done through the reverse β-oxidation pathway and is considered as VFA upgrading when the starting electron acceptor is produced from the organic feedstock (through primary fermentation) as well as when it is externally fed to the reactor. This process is considered as ethanol upgrading when the starting electron acceptor is *in situ* produced through ethanol oxidation (into acetate).

[ii] This process is not only done through the reverse β-oxidation pathway but also through direct oxidation of ethanol (excessive ethanol oxidation; EEO)

Materials and methods for microbial community analysis

DNA extraction

Genomic DNA was extracted from granular and suspended sludge fractions (500 µl sludge per sample) using a Fast DNA SPIN kit for soil (MP Biomedicals, Solon, OH), according to the manufacturers' protocol. Bead beating was performed using a FastPrep instrument (MP Biomedicals).

Bacterial community analysis

Samples for bacterial community analysis were labelled according to the corresponding CO_2 loading rate and sludge type (see overview in Figure 3); the initial bacterial community was labelled as 'IBC' (I). At high CO_2 loading rate (2.5 $L_{CO2} \cdot L^{-1} \cdot d^{-1}$), granular sludge was labelled as '2.5 granular' (R1go) and suspended sludge was labelled as '2.5 suspended' (R1lo). At medium CO_2 loading rate (1.0 $L_{CO2} \cdot L^{-1} \cdot d^{-1}$), granular sludge was labelled as '1.0 granular' (R1g) and suspended sludge was labelled as '1.0 suspended' (R1l). At no CO_2 loading rate (0.0 $L_{CO2} \cdot L^{-1} \cdot d^{-1}$), granular sludge was labelled as '0.0 granular' (R1gx) and suspended sludge was labelled as '0.0 suspended' (R1lx). Mock communities were also added in the analysis as previously used [1]. Extracted DNA was subjected to amplification of the V1–V2 region of the 16S rRNA gene using primers 27F-DegS [2] and an equimolar mix of reverse primers 338R-I and 338R-II [3] that were extended with 18 bp Universal Tags (Unitags). All amplification and purification steps were done as described previously [4]. All PCR reactions were done in a Thermocycler (G-storm, Essex, UK). After purification, DNA was quantified using a Nanodrop 1000 spectrophotometer (Thermo Fisher Scientific, Waltham, MA). Purified PCR products were pooled in an equimolar mix, adapter-ligated and sequenced using the MiSeq platform (GATC-Biotech, Konstanz, Germany). Analysis of the sequenced data was done using NG-Tax, an in-house pipeline [1]. Operational taxonomic units (OTUs) were assigned with the NG-Tax default settings which are extensively described by Ramiro-Garcia et al. (2016) [1]. In short, barcoded-primer and chimera filtering was done and only read pairs with perfectly matching primers and barcodes were kept. OTU picking was done using a 97% cutoff value and a OTU table was generated using a minimum relative abundance threshold of 0.1%. This resulted in 23556 reads for the IBC sample, 160591 reads for sample '2.5 granular' (R1go), 38223 reads for sample '2.5 suspended' (R1lo), 59806 reads for sample '1.0 granular'(R1g), 208183 reads for sample '1.0

suspended' (R1l), 112817 reads for sample '0.0 granular' (R1gx), and 64301 reads for sample '0.0 suspended' (R1lx). The relative abundances per OTU were then calculated from the amount of reads of the OTU relative to the total amount of reads in the sample. Taxonomic assignment was done against the non-clustered, non-redundant SILVA 16S rRNA reference database [5] using the uclust algorithm [6]. Microbial composition plots were made with a workflow that is based on Quantitative Insights Into Microbial Ecology (QIIME) v1.8.0 [7]. The project was deposited to the SRA archive of the European Nucleotide Archive (ENA) with the study accession number PRJEB19881 (ERP021948) (http://www.ebi.ac.uk/).

Archaeal community analysis

For archaeal community profiling, extracted DNA was used for clone library construction. To amplify almost full-length archaeal 16S rRNA genes for cloning, the primer A109f (ACKGCTCAGTAACACGT) [8] and universal reverse primer 1492R (GYTACCTTGTTACGACTT) [9] were used. PCR amplification was done with a GoTaq polymerase kit (Promega, Madison, WI) and using a LabCycler Gradient (SensoQuest, Göttingen, Germany). The PCR program consisted of a pre-denaturing step of 30 s at 98 °C, followed by 25 cycles of 98 °C for 10 s, 56 °C for 20 s, and 72 °C for 20 s. Lastly, a post-elongation step of 10 min at 72 °C was done. PCR products were purified using a PCR Clean & Concentrator kit (Zymo Research Corporation, Irvine, CA) and ligated into the pGEM-T Easy plasmid vector (pGEM-T Easy vector system I; Promega), and transformed into Escherichia coli XL1-Blue competent cells (Stratagene/Agilent Technologies, Santa Clara, CA). Both ligation and transformation were performed according to the manufacturer's instructions. Afterwards, PCR was done using primers SP6 (ATTTAGGTGACACTATAG) and T7 (TAATACGACTCACTATAGGG) to amplify the cloned 16S rRNA plasmid inserts. The PCR program consisted of a pre-denaturing step of 2 min at 95 °C, followed by 25 cycles of 95 °C for 30 s, 55 °C for 40 s, and 72 °C for 1.3 min. Lastly, a post-elongation step of 5 min at 72 °C was done. PCR products were checked on an agarose gel and were sent for sequencing using the Sanger platform at GATC-Biotech (Konstanz, Germany). Forward and reverse partial sequences were assembled into full length 16S rRNA genes and trimmed for vector sequences and low quality sequences using the DNA sequence assembler of DNA Baser software (Heracle BioSoft SRL, Romania). Obtained full length 16S rRNA gene sequences were compared with 16S rRNA sequences (bacteria and archaea) using the NCBI BLAST search algorithm (http://blast.ncbi.nlm.nih.gov/Blast.cgi). The project was deposited to the European Nucleotide Archive (ENA) with study accession numbers LT855569-LT855663 (http://www.ebi.ac.uk/).

Table S2. Calculations on carbon fluxes and numerical values at high CO_2 loading rate (2.5 $L_{CO2}\cdot L^{-1}\cdot d^{-1}$) and at low CO_2 loading rate (0.5 $L_{CO2}\cdot L^{-1}\cdot d^{-1}$)

Process number	Description	Calculation on carbon flux	Carbon flux [mmol $C\cdot L^{-1}\cdot d^{-1}$]	
			2.5 $L_{CO2}\cdot L^{-1}\cdot d^{-1}$ [i]	0.5 $L_{CO2}\cdot L^{-1}\cdot d^{-1}$ [i]
I	Total CO_2 use	$1\cdot\lvert r_{CO2}\rvert$	100	20
I a	CO_2 use by methanogens	$1\cdot r_{CH4}$	73	17
I b	Unidentified CO_2 use (i.e. biomass)	1·(I - I a)	27	3
II	Total ethanol use	$2\cdot\lvert r_{Ethanol}\rvert$	1130	456
II a [ii]	Excessive ethanol oxidation (EEO)	II - II b - II c - II d	326	72
II b [iii]	Ethanol oxidation through the reverse β-oxidation pathway	1/5 · (II c + II d)	134	64
II c [iv]	Ethanol use for elongation of fatty acids through the reverse β-oxidation pathway (even)	$2\cdot(r_{Butyrate} + 2\cdot r_{Caproate} + 3\cdot r_{Caprylate})$	459	134
II d [iv]	Ethanol use for elongation of fatty acids through the reverse β-oxidation pathway (odd)	$2\cdot(r_{Valerate} + 2\cdot r_{Heptanoate})$	211	185
III	Propionate use for VFA upgrading	$3\cdot(r_{Valerate} + r_{Heptanoate})$	275	251
IV	(Interspecies) hydrogen transfer			
V	Acetate uptake for ethanol upgrading	$2\cdot(r_{Butyrate} + r_{Caproate} + r_{Caprylate})$	264	81
VI	Methane production	$1\cdot r_{CH4}$	73	17
VII	Hydrogen production			
VIII	Unidentified acetate use (i.e. biomass)	II a + II b - V - IX	102	5
IX	Acetate production	$2\cdot r_{Acetate}$	94	50
X	Butyrate, caproate and caprylate production	$4\cdot r_{Butyrate} + 6\cdot r_{Caproate} + 8\cdot r_{Caprylate}$	723	215
XI	Valerate and heptanoate production	$5\cdot r_{Valerate} + 7\cdot r_{Heptanoate}$	486	436

[i] The ethanol loading rate at 2.5 $L_{CO2}\cdot L^{-1}\cdot d^{-1}$ was 32.2 $g\cdot L^{-1}\cdot d^{-1}$ whereas the ethanol loading rate at 0.5 $L_{CO2}\cdot L^{-1}\cdot d^{-1}$ was 16.3 $g\cdot L^{-1}\cdot d^{-1}$. Yet, carbon fluxes are comparable because ethanol concentrations were similar.

[ii] Excessive ethanol oxidation (EEO) is the use of ethanol that is not done by the reverse β-oxidation pathway (II b, II c & II d)

[iii] Ethanol oxidation into acetate by the reverse β-oxidation pathway is $1/5^{th}$ times ethanol use for elongation of fatty acids (II c + II d)

[iv] Ethanol that is used for elongation of fatty acids by reverse β-oxidation pathway is a function of elongation steps per net produced fatty acid. This is 1 step for butyrate and valerate, 2 steps for caproate and heptanoate and 3 steps for caprylate

r_x values are net production or consumption rates in $mmol\cdot L^{-1}\cdot d^{-1}$

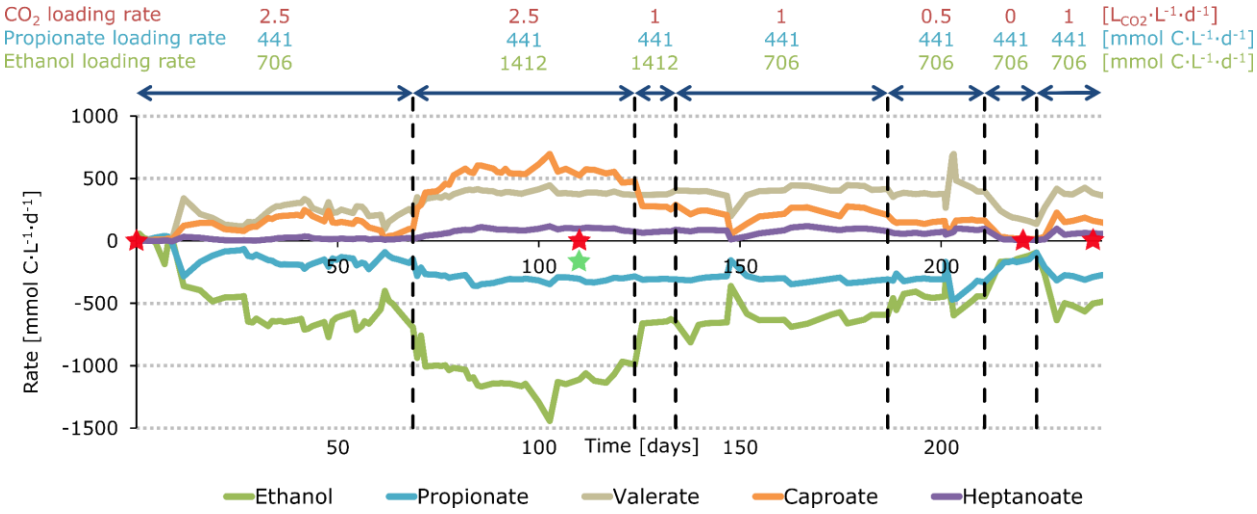

Figure S1. Graphical summary of the effect of CO_2 loading rate on reactor performance with net production and consumption rates over time. At the red stars, samples for bacterial community analysis were taken. At the green star, a sample for archaeal community analysis was taken. T = 30 °C, pH = 6.8, HRT = 17 h, V = 1 L

Mean steady state values of reactor concentrations, rates and carbon selectivities

Table S3. Mean steady state values at 2.5 $L_{CO2} \cdot L^{-1} \cdot d^{-1}$; day 84-97, 105-119

Compound	Concentration [mmol·L^{-1}]	Rate [mmol·L^{-1}·d^{-1}]	Selectivity [mol C %]
Ethanol	81.3 ± 30.1	-565 ± 15.3	N.A.
Propanol	9.1 ± 1.4	14.1 ± 3.0	2.7
Acetate	31.8 ± 1.5	46.9 ± 2.2	6.1
Propionate	28.4 ± 2.3	-106.6 ± 7.3	N.A.
Butyrate	24.9 ± 1.9	36.5 ± 2.5	9.4
Valerate	52.9 ± 1.1	77.9 ± 2.3	25.1
Caproate	63.4 ± 1.6	93.3 ± 3.9	36.1
Heptanoate	9.3 ± 0.5	13.8 ± 1.1	6.2
Caprylate	1.5 ± 0.4	2.1 ± 0.7	1.1
CO_2	4.6 ± 0.2 %	-99.8 ± 5.3	N.A.
CH_4	91.9 ± 0.2 %	72.6 ± 0.2	4.7
H_2	0.03 ± 0.01 %		N.A.
Unidentified			8.5

Table S4. Mean steady state values at 1.0 $L_{CO2} \cdot L^{-1} \cdot d^{-1}$; day 155-187

Compound	Concentration [mmol·L^{-1}]	Rate [mmol·L^{-1}·d^{-1}]	Selectivity [mol C %]
Ethanol	15.6 ± 10.2	-323.3 ± 29.8	N.A.
Propanol	4.8 ± 1.5	7.7 ± 2.2	2.3
Acetate	21.5 ± 2.8	30.1 ± 3.9	6.0
Propionate	30.0 ± 3.0	-104.6 ± 5.6	N.A.
Butyrate	15 ± 0.7	21.6 ± 1.1	8.7
Valerate	57.4 ± 2.3	82.9 ± 3.9	41.6
Caproate	26.8 ± 2.6	39.7 ± 5.2	23.9
Heptanoate	8.8 ± 1.4	12.8 ± 2	9.0
Caprylate	0.7 ± 0.1	1.0 ± 0.3	0.8
CO_2	2.3 ± 0.2 %	-36.9 ± 3.7	N.A.
CH_4	92.2 ± 0.6 %	34.3 ± 0.2	3.4
H_2	0.08 ± 0.04 %		N.A.
Unidentified			4.2

Selectivity (mol C%) = mol C product/mol C total consumed substrates · 100
N.A. = Not Applicable
Concentrations of gaseous compounds (CO_2, CH_4, H_2) are shown as % in headspace at 1 atm

Table S5. Mean steady state values at 0.5 $L_{CO2} \cdot L^{-1} \cdot d^{-1}$; day 188-201

Compound	Concentration [mmol·L^{-1}]	Rate [mmol·L^{-1}·d^{-1}]	Selectivity [mol C %]
Ethanol	70.1 ± 25.6	-227.8 ± 23.5	N.A.
Propanol	12.9 ± 1.0	19.7 ± 2.2	7.6
Acetate	18.5 ± 1.4	25.0 ± 4.5	6.4
Propionate	30.9 ± 2.0	-101.1 ± 6.7	N.A.
Butyrate	11.0 ± 0.6	14.8 ± 1.2	7.6
Valerate	54.3 ± 1.4	74.6 ± 2.2	47.9
Caproate	18.6 ± 1.8	25.0 ± 1.5	19.3
Heptanoate	6.6 ± 0.7	9.0 ± 0.9	8.1
Caprylate	0.6 ± 0.2	0.7 ± 0.5	0.8
CO_2	1.1 %	-19.9	N.A.
CH_4	87.9 %	17.1	2.2
H_2	0.2 %		N.A.
Unidentified			0.2

Table S6. Mean values at 0 $L_{CO2} \cdot L^{-1} \cdot d^{-1}$; day 216-222 (No steady state)

Compound	Concentration [mmol·L^{-1}]	Rate [mmol·L^{-1}·d^{-1}]	Selectivity [mol C %]
Ethanol	188.5 ± 15.7	-75.6 ± 10	N.A.
Propanol	8.9 ± 1.2	12.3 ± 1.5	11.7
Acetate	12.2 ± 0.8	17.1 ± 0.8	10.9
Propionate	67.7 ± 3.3	-54.6 ± 3.3	N.A.
Butyrate	5.0 ± 0.7	6.9 ± 0.9	8.7
Valerate	27.8 ± 4.0	38.1 ± 4.7	60.4
Caproate	3.0 ± 0.9	3.6 ± 0.8	6.9
Heptanoate	1.3 ± 0.4	1.4 ± 0.1	3.2
Caprylate	0.4 ± 0.1	0.5 ± 0.5	1.2
CO_2	0.07 ± 0.01 %	0 ± 0	N.A.
CH_4	49.3 ± 3.9 %	1.5 ± 0.1	0.5
H_2	41.6 ± 5.1 %		N.A.
Unidentified			-3.4

Selectivity (mol C%) = mol C product/mol C total consumed substrates · 100
N.A. = Not Applicable
Concentrations of gaseous compounds (CO_2, CH_4, H_2) are shown as % in headspace at 1 atm

Table S7. Mean steady state values at 1.0 $L_{CO2} \cdot L^{-1} \cdot d^{-1}$; day 229-240

Compound	Concentration [$mmol \cdot L^{-1}$]	Rate [$mmol \cdot L^{-1} \cdot d^{-1}$]	Selectivity [mol C %]
Ethanol	56.7 ± 15	-267.2 ± 28.1	N.A.
Propanol	6.4 ± 0.7	9.5 ± 1.6	3.3
Acetate	27.9 ± 2.5	42.5 ± 4.6	9.8
Propionate	39.3 ± 2.9	-97.2 ± 6.2	N.A.
Butyrate	12.9 ± 0.4	19.7 ± 0.7	9.1
Valerate	51.9 ± 1.9	78 ± 5.1	45.1
Caproate	18.9 ± 1.9	28.7 ± 4.9	19.9
Heptanoate	6.1 ± 1.1	9.2 ± 2.4	7.4
Caprylate	0.7 ± 0.1	1.0 ± 0.3	0.9
CO_2	1.4 ± 0.01 %	-38.7 ± 0.3	N.A.
CH_4	93.1 ± 0.5 %	29.6 ± 0.1	3.4
H_2	0.1 ± 0.005 %		N.A.
Unidentified			0.9

Selectivity (mol C%) = mol C product/mol C total consumed substrates · 100
N.A. = Not Applicable
Concentrations of gaseous compounds (CO_2, CH_4, H_2) are shown as % in headspace at 1 atm

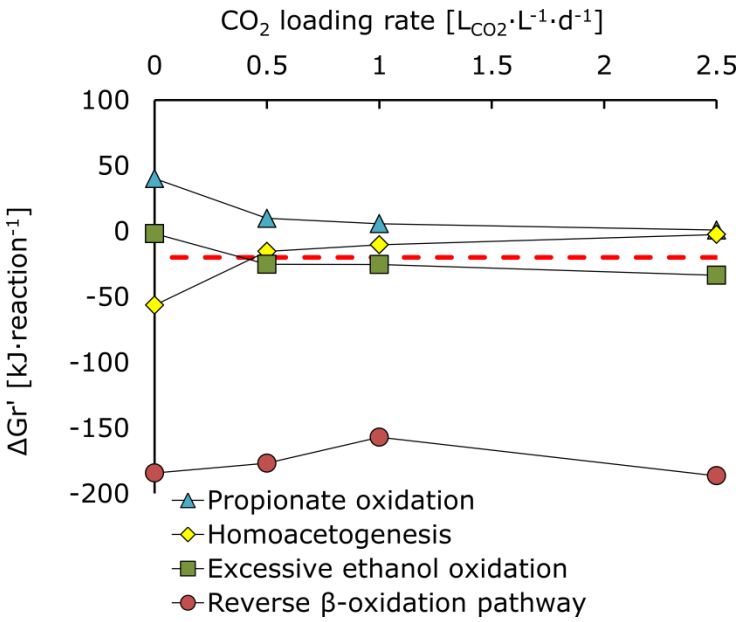

Figure S2. Results of thermodynamic analysis: change in Gibbs free energy of propionate oxidation (process 5, Table S1), homoacetogenesis (eq 6, Table S1), excessive ethanol oxidation (EEO; eq 1a, Table S1), reverse *β*-oxidation pathway (ethanol oxidation coupled to 5x propionate elongation; eq 1b + 2a, Table S1) at different CO_2 loading rates under actual bioreactor conditions (pH = 6.8, T = 30°C, steady state concentrations of substrates and products). The red line indicates the thermodynamic feasible limit of -20 kJ·reaction^{-1} for microorganisms [10].

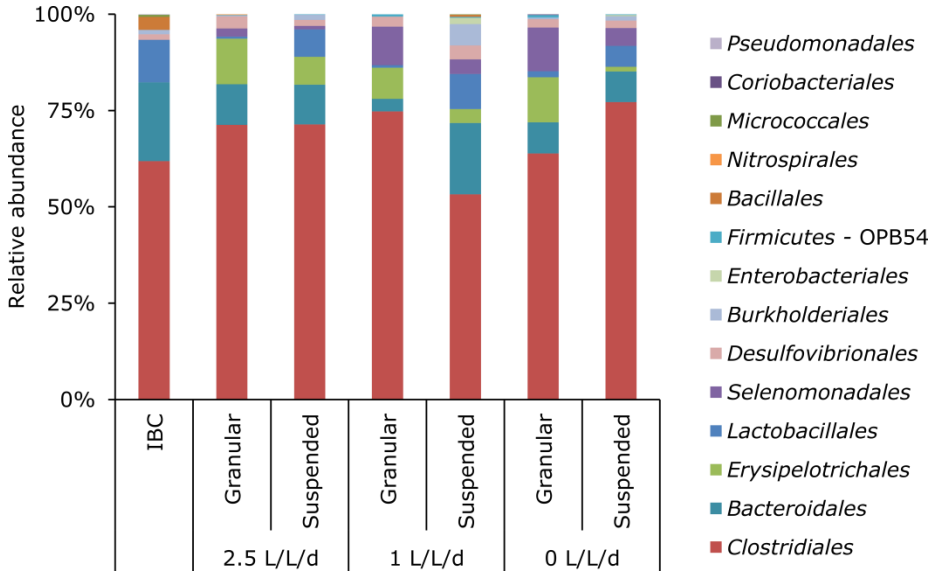

Figure S3. Results of bacterial community analysis: order level composition of bacterial community at different CO_2 loading rates in granular and suspended sludge. IBC = initial bacterial community

Table S8. Results of archaeal community analysis: phylogenetic affiliation of the cloned 16S rRNA gene sequences from the archaeal community in suspended sludge at 2.5 $L_{CO2} \cdot L^{-1} \cdot d^{-1}$

Closest cultured relative	No. of clones	Sequence identity [%]
Methanobrevibacter acididurans	58	99
Methanobrevibacter acididurans	31	98
Methanobrevibacter acididurans	6	97
Failed clones	1	
Total no. of clones	96	

References

1. Ramiro-Garcia, J.; Hermes, G.; Giatsis, C.; Sipkema, D.; Zoetendal, E.; Schaap, P.; Smidt, H., NG-Tax, a highly accurate and validated pipeline for analysis of 16S rRNA amplicons from complex biomes [version 1; referees: 2 approved with reservations, 1 not approved]. *F1000Research* **2016,** *5* (1791).
2. van den Bogert, B.; de Vos, W. M.; Zoetendal, E. G.; Kleerebezem, M., Microarray analysis and barcoded pyrosequencing provide consistent microbial profiles depending on the source of human intestinal samples. *Appl. Environ. Microbiol.* **2011,** *77* (6), 2071-2080.
3. Daims, H.; Brühl, A.; Amann, R.; Schleifer, K.-H.; Wagner, M., The domain-specific probe EUB338 is insufficient for the detection of all Bacteria: development and evaluation of a more comprehensive probe set. *Syst. Appl. Microbiol.* **1999,** *22* (3), 434-444.
4. Lu, Y.; Ramiro-Garcia, J.; Vandermeeren, P.; Herrmann, S.; Cichocka, D.; Springael, D.; Atashgahi, S.; Smidt, H., Dechlorination of three tetrachlorobenzene isomers by contaminated harbor sludge-derived enrichment cultures follows thermodynamically favorable reactions. *Appl. Microbiol. Biotechnol.* **2017,** *101* (6), 2589-2601.
5. Quast, C.; Pruesse, E.; Yilmaz, P.; Gerken, J.; Schweer, T.; Yarza, P.; Peplies, J.; Glöckner, F. O., The SILVA ribosomal RNA gene database project: improved data processing and web-based tools. *Nucleic Acids Res.* **2013,** *41* (Database issue), D590-D596.
6. Edgar, R. C., Search and clustering orders of magnitude faster than BLAST. *Bioinf.* **2010,** *26* (19), 2460-2461.
7. Caporaso, J. G.; Kuczynski, J.; Stombaugh, J.; Bittinger, K.; Bushman, F. D.; Costello, E. K.; Fierer, N.; Peña, A. G.; Goodrich, J. K.; Gordon, J. I.; Huttley, G. A.; Kelley, S. T.; Knights, D.; Koenig, J. E.; Ley, R. E.; Lozupone, C. A.; McDonald, D.; Muegge, B. D.; Pirrung, M.; Reeder, J.; Sevinsky, J. R.; Turnbaugh, P. J.; Walters, W. A.; Widmann, J.; Yatsunenko, T.; Zaneveld, J.; Knight, R., QIIME allows analysis of high-throughput community sequencing data. *Nat. Methods* **2010,** *7* (5), 335-336.
8. Großkopf, R.; Janssen, P. H.; Liesack, W., Diversity and structure of the methanogenic community in anoxic rice paddy soil microcosms as examined by cultivation and direct 16S rRNA gene sequence retrieval. *Appl. Environ. Microbiol.* **1998,** *64* (3), 960-969.
9. Lane, D. J., 16S/23S rRNA sequencing. In *Nucleic acid techniques in bacterial systematics*, Stackebrandt, E.; Goodfellow , M., Eds. John Wiley & Sons, Inc.: New York, NY, 1991; pp 115-175.
10. Schink, B., Energetics of syntrophic cooperation in methanogenic degradation. *Microbiol. Mol. Biol. Rev.* **1997,** *61* (2), 262-280.